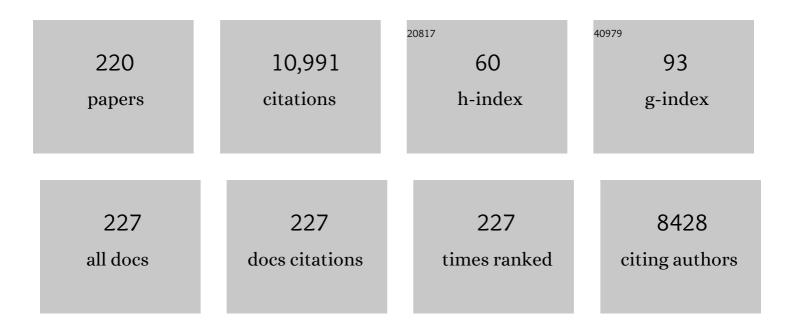
List of Publications by Year in descending order

Source: https://exaly.com/author-pdf/5488109/publications.pdf Version: 2024-02-01



FENC DENC

#	Article	IF	CITATIONS
1	Au-ZSM-5 catalyses the selective oxidation of CH4 to CH3OH and CH3COOH using O2. Nature Catalysis, 2022, 5, 45-54.	34.4	95
2	Application of solid-state NMR techniques for structural characterization of metal-organic frameworks. Solid State Nuclear Magnetic Resonance, 2022, 117, 101772.	2.3	14
3	Mechanistic Insight into Ethanol Dehydration over SAPO-34 Zeolite by Solid-state NMR Spectroscopy. Chemical Research in Chinese Universities, 2022, 38, 155-160.	2.6	8
4	Preferential adsorption sites for propane/propylene separation on ZIF-8 as revealed by solid-state NMR spectroscopy. Physical Chemistry Chemical Physics, 2022, 24, 6535-6543.	2.8	4
5	Identifying Crystallographically Different Siâ^'OHâ^'Al BrÃ,nsted Acid Sites in LTA Zeolites. Angewandte Chemie - International Edition, 2022, 61, .	13.8	6
6	Aluminum-Doped TiO <sub>2</sub> with Dominant {001} Facets: Microstructure and Property Evolution and Photocatalytic Activity. Journal of Physical Chemistry C, 2022, 126, 5555-5563.	3.1	7
7	Heterogeneous parahydrogen induced polarization on Rh-containing silicalite-1 zeolites: effect of the catalyst structure on signal enhancement. Catalysis Science and Technology, 2022, 12, 4442-4449.	4.1	2
8	Dynamic Self-Dispersion of Aggregated Boron Clusters into Stable Oligomeric Boron Species on MFI Zeolite Nanosheets under Oxidative Dehydrogenation of Propane. ACS Catalysis, 2022, 12, 7368-7376.	11.2	13
9	Throughâ€space 11 B– 27 Al correlation: Influence of the recoupling channel. Magnetic Resonance in Chemistry, 2021, 59, 1062-1076.	1.9	3
10	Dual Active Sites on Molybdenum/ZSMâ€5 Catalyst for Methane Dehydroaromatization: Insights from Solidâ€6tate NMR Spectroscopy. Angewandte Chemie, 2021, 133, 10804-10810.	2.0	2
11	Influence of Trimethylphosphine Oxide Loading on the Measurement of Zeolite Acidity by Solid-State NMR Spectroscopy. Journal of Physical Chemistry C, 2021, 125, 9497-9506.	3.1	15
12	Dual Active Sites on Molybdenum/ZSMâ€5 Catalyst for Methane Dehydroaromatization: Insights from Solidâ€6tate NMR Spectroscopy. Angewandte Chemie - International Edition, 2021, 60, 10709-10715.	13.8	39
13	Interfacial-Bonding Ti–N–C Boosts Efficient Photocatalytic H <sub>2</sub> Evolution in Close Coupling g-C <sub>3</sub> N <sub>4</sub> /TiO <sub>2</sub> . Journal of Physical Chemistry C, 2021, 125, 12012-12018.	3.1	11
14	Hostâ€Guest Interaction in Ethylene and Ethane Separation on Zeolitic Imidazolate Frameworks as Revealed by Solidâ€ <del>S</del> tate NMR Spectroscopy. Chemistry - A European Journal, 2021, 27, 11303-11308.	3.3	7
15	Pairwise Stereoselective Hydrogenation of Propyne on Supported Pd–Ag Catalysts Investigated by Parahydrogen-Induced Polarization. Journal of Physical Chemistry C, 2021, 125, 17144-17154.	3.1	6
16	Efficient and selective photocatalytic CH4 conversion to CH3OH with O2 by controlling overoxidation on TiO2. Nature Communications, 2021, 12, 4652.	12.8	131
17	Stabilizing the framework of SAPO-34 zeolite toward long-term methanol-to-olefins conversion. Nature Communications, 2021, 12, 4661.	12.8	32
18	Unraveling Hydrocarbon Pool Boosted Propane Aromatization on Gallium/ZSMâ€5 Zeolite by Solidâ€5tate Nuclear Magnetic Resonance Spectroscopy. Angewandte Chemie, 2021, 133, 23822-23826.	2.0	1

#	Article	IF	CITATIONS
19	Breathing Effect via Solvent Inclusions on the Linker Rotational Dynamics of Functionalized MILâ€53. Chemistry - A European Journal, 2021, 27, 14711-14720.	3.3	9
20	Unraveling Hydrocarbon Pool Boosted Propane Aromatization on Gallium/ZSMâ€5 Zeolite by Solidâ€5tate Nuclear Magnetic Resonance Spectroscopy. Angewandte Chemie - International Edition, 2021, 60, 23630-23634.	13.8	15
21	Solid-state NMR studies of internuclear correlations for characterizing catalytic materials. Chemical Society Reviews, 2021, 50, 8382-8399.	38.1	37
22	Insight into Carbocationâ€Induced Noncovalent Interactions in the Methanolâ€toâ€Olefins Reaction over ZSMâ€5 Zeolite by Solidâ€State NMR Spectroscopy. Angewandte Chemie - International Edition, 2021, 60, 26847-26854.	13.8	9
23	Titelbild: Insight into Carbocationâ€Induced Noncovalent Interactions in the Methanolâ€toâ€Olefins Reaction over ZSMâ€5 Zeolite by Solidâ€5tate NMR Spectroscopy (Angew. Chem. 51/2021). Angewandte Chemie, 2021, 133, 26617-26617.	2.0	0
24	Solidâ€state NMR studies of the acidity of functionalized metal–organic framework UiOâ€66 materials. Magnetic Resonance in Chemistry, 2020, 58, 1091-1098.	1.9	7
25	Mechanism of Methanolâ€toâ€hydrocarbon Reaction over Zeolites: A solidâ€state NMR Perspective. ChemCatChem, 2020, 12, 965-980.	3.7	33
26	Solid-state 31P NMR mapping of active centers and relevant spatial correlations in solid acid catalysts. Nature Protocols, 2020, 15, 3527-3555.	12.0	54
27	Quantitative Analysis of Linker Composition and Spatial Arrangement of Multivariate Metal–Organic Framework UiO-66 through <sup>1</sup> H Fast MAS NMR. Journal of Physical Chemistry C, 2020, 124, 17640-17647.	3.1	12
28	Mapping the oxygen structure of $\hat{l}^3$ -Al2O3 by high-field solid-state NMR spectroscopy. Nature Communications, 2020, 11, 3620.	12.8	42
29	Probing the active sites for methane activation on Ga/ZSM-5 zeolites with solid-state NMR spectroscopy. Chemical Communications, 2020, 56, 12029-12032.	4.1	5
30	Hydrogen Spillover to Oxygen Vacancy of TiO <sub>2–<i>x</i></sub> H <sub><i>y</i></sub> /Fe: Breaking the Scaling Relationship of Ammonia Synthesis. Journal of the American Chemical Society, 2020, 142, 17403-17412.	13.7	91
31	Recent Advances of Solidâ€State NMR Spectroscopy for Microporous Materials. Advanced Materials, 2020, 32, e2002879.	21.0	50
32	Molecular Vises for Precisely Positioning Ligands near Catalytic Metal Centers in Metal–Organic Frameworks. Journal of the American Chemical Society, 2020, 142, 16182-16187.	13.7	29
33	Evolution of D6R units in the interzeolite transformation from FAU, MFI or *BEA into AEI: transfer or reassembly?. Inorganic Chemistry Frontiers, 2020, 7, 2204-2211.	6.0	47
34	gem â€Diolâ€Type Intermediate in the Activation of a Ketone on Snâ€Î² Zeolite as Studied by Solidâ€State NMR Spectroscopy. Angewandte Chemie, 2020, 132, 19700-19706.	2.0	2
35	gem â€Ðiolâ€Type Intermediate in the Activation of a Ketone on Snâ€Î² Zeolite as Studied by Solidâ€5tate NMR Spectroscopy. Angewandte Chemie - International Edition, 2020, 59, 19532-19538.	13.8	13
36	Theoretical Prediction from Classical Equations and Rational Synthesis of Ultrafine LTL Zeolite Nanocrystals. Journal of Physical Chemistry C, 2020, 124, 13819-13824.	3.1	2

#	Article	IF	CITATIONS
37	Synthesis of Aluminophosphate Molecular Sieves in Alkaline Media. Chemistry - A European Journal, 2020, 26, 11408-11411.	3.3	5
38	Establishing a Link Between the Dual Cycles in Methanol-to-Olefins Conversion on H-ZSM-5: Aromatization of Cycloalkenes. ACS Catalysis, 2020, 10, 4299-4305.	11.2	29
39	A Hydrothermally Stable Irreducible Oxideâ€Modified Pd/MgAl <sub>2</sub> O <sub>4</sub> Catalyst for Methane Combustion. Angewandte Chemie, 2020, 132, 18680-18684.	2.0	14
40	A Hydrothermally Stable Irreducible Oxideâ€Modified Pd/MgAl <sub>2</sub> O <sub>4</sub> Catalyst for Methane Combustion. Angewandte Chemie - International Edition, 2020, 59, 18522-18526.	13.8	64
41	Primary Adsorption Sites of Light Alkanes in Multivariate UiO-66 at Room Temperature as Revealed by Solid-State NMR. Journal of Physical Chemistry C, 2020, 124, 3738-3746.	3.1	12
42	Ï€â€Interactions between Cyclic Carbocations and Aromatics Cause Zeolite Deactivation in Methanolâ€ŧoâ€Hydrocarbon Conversion. Angewandte Chemie, 2020, 132, 7265-7269.	2.0	7
43	Surface Water Loading on Titanium Dioxide Modulates Photocatalytic Water Splitting. Cell Reports Physical Science, 2020, 1, 100013.	5.6	17
44	Ï€â€Interactions between Cyclic Carbocations and Aromatics Cause Zeolite Deactivation in Methanolâ€ŧoâ€Hydrocarbon Conversion. Angewandte Chemie - International Edition, 2020, 59, 7198-7202.	13.8	35
45	Solid-state NMR for metal-containing zeolites: From active sites to reaction mechanism. Frontiers of Chemical Science and Engineering, 2020, 14, 159-187.	4.4	18
46	Hydroiodic Acid Additive Enhanced the Performance and Stability of PbS-QDs Solar Cells via Suppressing Hydroxyl Ligand. Nano-Micro Letters, 2020, 12, 37.	27.0	35
47	Multiple Methane Activation Pathways on Gaâ€modified ZSMâ€5 Zeolites Revealed by Solidâ€6tate NMR Spectroscopy. ChemCatChem, 2020, 12, 3880-3889.	3.7	7
48	Sustainable Synthesis of Pure Silica Zeolites from a Combined Strategy of Zeolite Seeding and Alcohol Filling. Angewandte Chemie - International Edition, 2019, 58, 12138-12142.	13.8	47
49	Sustainable Synthesis of Pure Silica Zeolites from a Combined Strategy of Zeolite Seeding and Alcohol Filling. Angewandte Chemie, 2019, 131, 12266-12270.	2.0	3
50	Beyond the Thermal Equilibrium Limit of Ammonia Synthesis with Dual Temperature Zone Catalyst Powered by Solar Light. CheM, 2019, 5, 2702-2717.	11.7	91
51	The acidic nature of "NMR-invisible―tri-coordinated framework aluminum species in zeolites. Chemical Science, 2019, 10, 10159-10169.	7.4	78
52	Host–Guest Interaction between Methanol and Metal–Organic Framework Cu <sub>3–<i>x</i></sub> Zn <sub><i>x</i></sub> (btc) <sub>2</sub> as Revealed by Solid-State NMR. Journal of Physical Chemistry C, 2019, 123, 24062-24070.	3.1	12
53	Boosting the turnover number of core–shell Al-ZSM-5@B-ZSM-5 zeolite for methanol to propylene reaction by modulating its gradient acid site distribution and low consumption diffusion. Catalysis Science and Technology, 2019, 9, 659-671.	4.1	33
54	Origin of High Selectivity of Dimethyl Ether Carbonylation in the 8-Membered Ring Channel of Mordenite Zeolite. Journal of Physical Chemistry C, 2019, 123, 15503-15512.	3.1	28

#	Article	IF	CITATIONS
55	Solid-State NMR Principles and Techniques. Lecture Notes in Quantum Chemistry II, 2019, , 1-55.	0.3	3
56	Metal Active Sites and Their Catalytic Functions in Zeolites: Insights from Solid-State NMR Spectroscopy. Accounts of Chemical Research, 2019, 52, 2179-2189.	15.6	106
57	Solid-State NMRÂCharacterization of Acid PropertiesÂofÂZeolites and Solid Acid Catalysts. Lecture Notes in Quantum Chemistry II, 2019, , 159-197.	0.3	5
58	Solid-State NMR in Zeolite Catalysis. Lecture Notes in Quantum Chemistry II, 2019, , .	0.3	17
59	In Situ Solid-State NMR Investigation of Catalytic Reactions on Zeolites. Lecture Notes in Quantum Chemistry II, 2019, , 199-254.	0.3	2
60	Solid-State NMRÂCharacterization of Host-Guest Interactions. Lecture Notes in Quantum Chemistry II, 2019, , 133-157.	0.3	1
61	Observation of an oxonium ion intermediate in ethanol dehydration to ethene on zeolite. Nature Communications, 2019, 10, 1961.	12.8	40
62	Isolated π-Interaction Sites in Mesoporous MOF Backbone for Repetitive and Reversible Dynamics in Water. ACS Applied Materials & Interfaces, 2019, 11, 973-981.	8.0	25
63	Direct observation of tin sites and their reversible interconversion in zeolites by solid-state NMR spectroscopy. Communications Chemistry, 2018, 1, .	4.5	54
64	Efficient synthesis of aluminosilicate RTH zeolite with good catalytic performances in NH <sub>3</sub> -SCR and MTO reactions. Journal of Materials Chemistry A, 2018, 6, 8705-8711.	10.3	22
65	Synthesis of EUâ€1/ZSMâ€48 Coâ€Crystalline Zeolites from Highâ€Silica EUâ€1 Seeds: Tailoring Phase Proportio and Promoting Long Crystallineâ€Phase Stability. Chemistry - A European Journal, 2018, 24, 6595-6605.	ns 3.3	13
66	Tuning Pd–Au Bimetallic Catalysts for Heterogeneous Parahydrogen-Induced Polarization. Journal of Physical Chemistry C, 2018, 122, 1248-1257.	3.1	13
67	Host-guest interaction of styrene and ethylbenzene in MIL-53 studied by solid-state NMR. Solid State Nuclear Magnetic Resonance, 2018, 90, 1-6.	2.3	13
68	Porous Organic Polymers Constructed from Tröger's Base as Efficient Carbon Dioxide Adsorbents and Heterogeneous Catalysts. ChemCatChem, 2018, 10, 1900-1904.	3.7	11
69	Enhanced Photocatalytic Performance of Carbon-Coated TiO <sub>2–<i>x</i></sub> with Surface-Active Carbon Species. Journal of Physical Chemistry C, 2018, 122, 10948-10955.	3.1	21
70	BrÃ,nsted/Lewis Acid Synergy in Methanol-to-Aromatics Conversion on Ga-Modified ZSM-5 Zeolites, As Studied by Solid-State NMR Spectroscopy. ACS Catalysis, 2018, 8, 69-74.	11.2	107
71	Methanol to Olefins Reaction over Cavity-type Zeolite: Cavity Controls the Critical Intermediates and Product Selectivity. ACS Catalysis, 2018, 8, 10950-10963.	11.2	59
72	A Mechanistic Study of Methanol-to-Aromatics Reaction over Ga-Modified ZSM-5 Zeolites: Understanding the Dehydrogenation Process. ACS Catalysis, 2018, 8, 9809-9820.	11.2	100

#	Article	IF	CITATIONS
73	Construction of Porous Aromatic Frameworks with Exceptional Porosity via Building Unit Engineering. Advanced Materials, 2018, 30, e1804169.	21.0	66
74	Probing the surface of γ-Al <sub>2</sub> O <sub>3</sub> by oxygen-17 dynamic nuclear polarization enhanced solid-state NMR spectroscopy. Physical Chemistry Chemical Physics, 2018, 20, 17218-17225.	2.8	29
75	Extraâ€Framework Aluminumâ€Assisted Initial Câ^'C Bond Formation in Methanolâ€toâ€Olefins Conversion on Zeolite Hâ€ZSMâ€5. Angewandte Chemie - International Edition, 2018, 57, 10197-10201.	13.8	86
76	Extraâ€Framework Aluminumâ€Assisted Initial Câ^'C Bond Formation in Methanolâ€ŧoâ€Olefins Conversion on Zeolite Hâ€ZSMâ€5. Angewandte Chemie, 2018, 130, 10354-10358.	2.0	23
77	New insights into the di- <i>n</i> -propylamine (DPA) molecule as an organic structural directing agent (OSDA) in the crystallization of AlPO <sub>4</sub> -11 molecular sieve. Inorganic Chemistry Frontiers, 2018, 5, 1633-1639.	6.0	10
78	Formation of aluminum diphosphonate mesostructures: The effect of aluminum source. Journal of Colloid and Interface Science, 2018, 532, 718-726.	9.4	0
79	Uniform signal enhancement in MAS NMR of half-integer quadrupolar nuclei using quadruple-frequency sweeps. Journal of Magnetic Resonance, 2018, 293, 92-103.	2.1	11
80	Facet dependent pairwise addition of hydrogen over Pd nanocrystal catalysts revealed via NMR using para-hydrogen-induced polarization. Physical Chemistry Chemical Physics, 2017, 19, 9349-9353.	2.8	16
81	Heteronuclear correlation experiments of 23Na-27Al in rotating solids. Solid State Nuclear Magnetic Resonance, 2017, 84, 103-110.	2.3	11
82	An NMR Scale for Measuring the Base Strength of Solid Catalysts with Pyrrole Probe: A Combined Solid-State NMR Experiment and Theoretical Calculation Study. Journal of Physical Chemistry C, 2017, 121, 3887-3895.	3.1	27
83	Understanding Surface and Interfacial Chemistry in Functional Nanomaterials via Solidâ€State NMR. Advanced Materials, 2017, 29, 1605895.	21.0	91
84	Solventâ€Free Synthesis of <scp>ITQ</scp> â€12, <scp>ITQ</scp> â€13, and <scp>ITQ</scp> â€17 Zeolites. Chir Journal of Chemistry, 2017, 35, 572-576.	iese 4.9	15
85	External or internal surface of H-ZSM-5 zeolite, which is more effective for the Beckmann rearrangement reaction?. Catalysis Science and Technology, 2017, 7, 2512-2523.	4.1	26
86	Highly efficient visible light induced photocatalytic activity of a novel in situ synthesized conjugated microporous poly(benzothiadiazole)–C <sub>3</sub> N <sub>4</sub> composite. Catalysis Science and Technology, 2017, 7, 418-426.	4.1	30
87	Solid-state NMR Studies of Host–Guest Interaction between UiO-67 and Light Alkane at Room Temperature. Journal of Physical Chemistry C, 2017, 121, 14261-14268.	3.1	25
88	Identification of double four-ring units in germanosilicate ITQ-13 zeolite by solid-state NMR spectroscopy. Solid State Nuclear Magnetic Resonance, 2017, 87, 1-9.	2.3	13
89	Carbonylation of ethane with carbon monoxide over Zn-modified ZSM-5 zeolites studied by in situ solid-state NMR spectroscopy. Journal of Catalysis, 2017, 345, 228-235.	6.2	20
90	<sup>31</sup> P NMR Chemical Shifts of Phosphorus Probes as Reliable and Practical Acidity Scales for Solid and Liquid Catalysts. Chemical Reviews, 2017, 117, 12475-12531.	47.7	258

#	Article	IF	CITATIONS
91	Host–Guest Interactions and Their Catalytic Consequences in Methanol to Olefins Conversion on Zeolites Studied by <sup>13</sup> C– <sup>27</sup> Al Double-Resonance Solid-State NMR Spectroscopy. ACS Catalysis, 2017, 7, 6094-6103.	11.2	24
92	Structure-directing effect on synthesis of layered aluminophosphates with same topology. Chemical Research in Chinese Universities, 2017, 33, 513-519.	2.6	4
93	Transfer Channel of Photoinduced Holes on a TiO <sub>2</sub> Surface As Revealed by Solid-State Nuclear Magnetic Resonance and Electron Spin Resonance Spectroscopy. Journal of the American Chemical Society, 2017, 139, 10020-10028.	13.7	96
94	A Hierarchical Bipyridineâ€Constructed Framework for Highly Efficient Carbon Dioxide Capture and Catalytic Conversion. ChemSusChem, 2017, 10, 1186-1192.	6.8	94
95	Direct Detection of Supramolecular Reaction Centers in the Methanolâ€toâ€Olefins Conversion over Zeolite Hâ€ZSMâ€5 by <sup>13</sup> C– <sup>27</sup> Al Solidâ€State NMR Spectroscopy. Angewandte Che 2016, 128, 2553-2557.	ന്നുക	14
96	Direct Detection of Supramolecular Reaction Centers in the Methanolâ€ŧoâ€Olefins Conversion over Zeolite Hâ€ZSMâ€5 by <sup>13</sup> C– <sup>27</sup> Al Solidâ€6tate NMR Spectroscopy. Angewandte Che International Edition, 2016, 55, 2507-2511.	miæ.8	67
97	Valence state alternation of copper species doped in HY zeolite as revealed by paramagnetic relaxation enhancement NMR spectroscopy. Solid State Nuclear Magnetic Resonance, 2016, 74-75, 10-15.	2.3	3
98	Mechanism of alkane H/D exchange over zeolite H-ZSM-5 at low temperature: a combined computational and experimental study. Catalysis Science and Technology, 2016, 6, 5350-5363.	4.1	18
99	An elaborate structure investigation of the chiral polymorph A-enriched zeolite beta. CrystEngComm, 2016, 18, 1782-1789.	2.6	19
100	Rücktitelbild: Direct Detection of Supramolecular Reaction Centers in the Methanolâ€toâ€Olefins Conversion over Zeolite Hâ€ZSMâ€5 by <sup>13</sup> C– <sup>27</sup> Al Solidâ€State NMR Spectroscopy (Angew. Chem. 7/2016). Angewandte Chemie, 2016, 128, 2648-2648.	2.0	0
101	Insights of the Crystallization Process of Molecular Sieve AlPO <sub>4</sub> -5 Prepared by Solvent-Free Synthesis. Journal of the American Chemical Society, 2016, 138, 6171-6176.	13.7	77
102	Methanol carbonylation over copper-modified mordenite zeolite: A solid-state NMR study. Solid State Nuclear Magnetic Resonance, 2016, 80, 1-6.	2.3	26
103	Polarization Switching Induced by Slowing the Dynamic Swinglike Motion in a Flexible Organic Dielectric. Journal of Physical Chemistry C, 2016, 120, 27571-27576.	3.1	14
104	Synergic Effect of Active Sites in Zincâ€Modified ZSMâ€5 Zeolites as Revealed by Highâ€Field Solidâ€State NMR Spectroscopy. Angewandte Chemie - International Edition, 2016, 55, 15826-15830.	13.8	59
105	Synergic Effect of Active Sites in Zincâ€Modified ZSMâ€5 Zeolites as Revealed by Highâ€Field Solidâ€State NMR Spectroscopy. Angewandte Chemie, 2016, 128, 16058-16062.	2.0	12
106	Origin of Zeolite Confinement Revisited by Energy Decomposition Analysis. Journal of Physical Chemistry C, 2016, 120, 27349-27363.	3.1	12
107	Unravelling the Efficient Photocatalytic Activity of Boron-induced Ti3+ Species in the Surface Layer of TiO2. Scientific Reports, 2016, 6, 34765.	3.3	53
108	Temperature-dependence of the influence of the position-2-methyl group on the structure-directing effect of piperazine in the synthesis of open-framework aluminophosphates. Scientific Reports, 2016, 6, 22019.	3.3	4

#	Article	IF	CITATIONS
109	Insights into the reaction mechanism of propene H/D exchange over acidic zeolite catalysts from theoretical calculations. Catalysis Science and Technology, 2016, 6, 6328-6338.	4.1	9
110	Self-Assembly of Cetyltrimethylammonium Bromide and Lamellar Zeolite Precursor for the Preparation of Hierarchical MWW Zeolite. Chemistry of Materials, 2016, 28, 4512-4521.	6.7	88
111	Methanol to hydrocarbons reaction over Hβ zeolites studied by high resolution solid-state NMR spectroscopy: Carbenium ions formation and reaction mechanism. Journal of Catalysis, 2016, 335, 47-57.	6.2	57
112	Acidic Properties and Structure–Activity Correlations of Solid Acid Catalysts Revealed by Solid-State NMR Spectroscopy. Accounts of Chemical Research, 2016, 49, 655-663.	15.6	177
113	Bistable N–Hâ∢N hydrogen bonds for reversibly modulating the dynamic motion in an organic co-crystal. Physical Chemistry Chemical Physics, 2016, 18, 10868-10872.	2.8	20
114	Direct observation of methylcyclopentenyl cations (MCP <sup>+</sup> ) and olefin generation in methanol conversion over TON zeolite. Catalysis Science and Technology, 2016, 6, 89-97.	4.1	28
115	Population transfer HMQC for half-integer quadrupolar nuclei. Journal of Chemical Physics, 2015, 142, 094201.	3.0	29
116	Experimental Evidence on the Formation of Ethene through Carbocations in Methanol Conversion over Hâ€ZSMâ€5 Zeolite. Chemistry - A European Journal, 2015, 21, 12061-12068.	3.3	62
117	Strong or weak acid, which is more efficient for Beckmann rearrangement reaction over solid acid catalysts?. Catalysis Science and Technology, 2015, 5, 3675-3681.	4.1	32
118	Investigation of the Strong BrÃ,nsted Acidity in a Novel SAPO-type Molecular Sieve, DNL-6. Journal of Physical Chemistry C, 2015, 119, 2589-2596.	3.1	14
119	Paramagnetic relaxation enhancement solid-state NMR studies of heterogeneous catalytic reaction over HY zeolite using natural abundance reactant. Solid State Nuclear Magnetic Resonance, 2015, 66-67, 29-32.	2.3	8
120	Synthesis of chiral polymorph A-enriched zeolite Beta with an extremely concentrated fluoride route. Scientific Reports, 2015, 5, 11521.	3.3	43
121	F-assisted synthesis of a hierarchical ZSM-5 zeolite for methanol to propylene reaction: a b-oriented thinner dimensional morphology. RSC Advances, 2015, 5, 61354-61363.	3.6	52
122	Room temperature stable zinc carbonyl complex formed in zeolite ZSM-5 and its hydrogenation reactivity: a solid-state NMR study. Chemical Communications, 2015, 51, 9177-9180.	4.1	5
123	Mesoporous ZSM-5 Zeolite-Supported Ru Nanoparticles as Highly Efficient Catalysts for Upgrading Phenolic Biomolecules. ACS Catalysis, 2015, 5, 2727-2734.	11.2	147
124	Highly Efficient Heterogeneous Hydroformylation over Rh-Metalated Porous Organic Polymers: Synergistic Effect of High Ligand Concentration and Flexible Framework. Journal of the American Chemical Society, 2015, 137, 5204-5209.	13.7	292
125	Slight channel difference influences the reaction pathway of methanol-to-olefins conversion over acidic H-ZSM-22 and H-ZSM-12 zeolites. Catalysis Science and Technology, 2015, 5, 3507-3517.	4.1	51
126	Methylbenzene hydrocarbon pool in methanol-to-olefins conversion over zeolite H-ZSM-5. Journal of Catalysis, 2015, 332, 127-137.	6.2	88

#	Article	IF	CITATIONS
127	Observation of 1H–13C and 1H–1H proximities in a paramagnetic solid by NMR at high magnetic field under ultra-fast MAS. Journal of Magnetic Resonance, 2015, 251, 36-42.	2.1	8
128	Hydrothermal treatment on ZSM-5 extrudates catalyst for methanol to propylene reaction: Finely tuning the acidic property. Fuel Processing Technology, 2015, 129, 130-138.	7.2	112
129	Highly nitrogen-doped mesoscopic carbons as efficient metal-free electrocatalysts for oxygen reduction reactions. Journal of Materials Chemistry A, 2014, 2, 20030-20037.	10.3	37
130	Acidity Characterization of Solid Acid Catalysts by Solid-State 31P NMR of Adsorbed Phosphorus-Containing Probe Molecules. Annual Reports on NMR Spectroscopy, 2014, 81, 47-108.	1.5	20
131	Secondâ€Order Nonlinear Optical Switch of a New Hydrogenâ€Bonded Supramolecular Crystal with a High Laserâ€Induced Damage Threshold. Advanced Optical Materials, 2014, 2, 1199-1205.	7.3	55
132	High performance nanosheet-like silicoaluminophosphate molecular sieves: synthesis, 3D EDT structural analysis and MTO catalytic studies. Journal of Materials Chemistry A, 2014, 2, 17828-17839.	10.3	96
133	Alkylation of benzene with carbon monoxide over Zn/H-ZSM-5 zeolite studied using in situ solid-state NMR spectroscopy. Chemical Communications, 2014, 50, 11382-11384.	4.1	16
134	The temperature-dependence of the structure-directing effect of 2-methylpiperazine in the synthesis of open-framework aluminophosphates. RSC Advances, 2014, 4, 39011-39019.	3.6	9
135	In situ growth-etching approach to the preparation of hierarchically macroporous zeolites with high MTO catalytic activity and selectivity. Journal of Materials Chemistry A, 2014, 2, 17994-18004.	10.3	102
136	New Insight into the Hydrocarbonâ€Pool Chemistry of the Methanolâ€ŧoâ€Olefins Conversion over Zeolite Hâ€ZSMâ€5 from GCâ€MS, Solid‣tate NMR Spectroscopy, and DFT Calculations. Chemistry - A European Journal, 2014, 20, 12432-12443.	3.3	131
137	Capturing the Local Adsorption Structures of Carbon Dioxide in Polyamine-Impregnated Mesoporous Silica Adsorbents. Journal of Physical Chemistry Letters, 2014, 5, 3183-3187.	4.6	13
138	Host–Guest Interactions in Dealuminated HY Zeolite Probed by <sup>13</sup> C– <sup>27</sup> Al Solid-State NMR Spectroscopy. Journal of Physical Chemistry Letters, 2014, 5, 3068-3072.	4.6	31
139	Sustainable Synthesis of Zeolites without Addition of Both Organotemplates and Solvents. Journal of the American Chemical Society, 2014, 136, 4019-4025.	13.7	233
140	Alkylation of Benzene with Methane over ZnZSM-5 Zeolites Studied with Solid-State NMR Spectroscopy. Journal of Physical Chemistry C, 2013, 117, 4018-4023.	3.1	45
141	Acidity characterization of heterogeneous catalysts by solid-state NMR spectroscopy using probe molecules. Solid State Nuclear Magnetic Resonance, 2013, 55-56, 12-27.	2.3	62
142	Effect of Surface Acid Properties of Modified VOx/Al2O3 Catalysts on Methanol Selective Oxidation. Catalysis Letters, 2013, 143, 624-629.	2.6	7
143	Signal enhancement of J-HMQC experiments in solid-state NMR involving half-integer quadrupolar nuclei. Chemical Communications, 2013, 49, 6653.	4.1	34
144	Molecular engineering of microporous crystals: (VII) The molar ratio dependence of the structure-directing ability of piperazine in the crystallization of four aluminophosphates with open-frameworks. Microporous and Mesoporous Materials, 2013, 176, 112-122.	4.4	18

#	Article	IF	CITATIONS
145	Recent Advances of Solid-State NMR Studies on Zeolites. Annual Reports on NMR Spectroscopy, 2013, 78, 1-54.	1.5	34
146	Progress in development and application of solid-state NMR for solid acid catalysis. Chinese Journal of Catalysis, 2013, 34, 436-491.	14.0	33
147	A defect-based strategy for the preparation of mesoporous zeolite Y for high-performance catalytic cracking. Journal of Catalysis, 2013, 298, 102-111.	6.2	120
148	Low-Temperature Reactivity of Zn <sup>+</sup> lons Confined in ZSM-5 Zeolite toward Carbon Monoxide Oxidation: Insight from in Situ DRIFT and ESR Spectroscopy. Journal of the American Chemical Society, 2013, 135, 6762-6765.	13.7	80
149	Pore Selectivity for Olefin Protonation Reactions Confined inside Mordenite Zeolite: A Theoretical Calculation Study. Journal of Physical Chemistry C, 2013, 117, 2194-2202.	3.1	43
150	Insight into Dimethyl Ether Carbonylation Reaction over Mordenite Zeolite from in-Situ Solid-State NMR Spectroscopy. Journal of Physical Chemistry C, 2013, 117, 5840-5847.	3.1	98
151	Understanding the High Photocatalytic Activity of (B, Ag)-Codoped TiO <sub>2</sub> under Solar-Light Irradiation with XPS, Solid-State NMR, and DFT Calculations. Journal of the American Chemical Society, 2013, 135, 1607-1616.	13.7	230
152	Stability of the Reaction Intermediates of Ethylbenzene Disproportionation over Medium-Pore Zeolites with Different Framework Topologies: A Theoretical Investigation. Journal of Physical Chemistry C, 2013, 117, 23626-23637.	3.1	23
153	Direct Observation of Cyclic Carbenium Ions and Their Role in the Catalytic Cycle of the Methanolâ€toâ€Olefin Reaction over Chabazite Zeolites. Angewandte Chemie - International Edition, 2013, 52, 11564-11568.	13.8	193
154	Amine Surface Modifications and Fluorescent Labeling of Thermally Stabilized Mesoporous Silicon Nanoparticles. Journal of Physical Chemistry C, 2012, 116, 22307-22314.	3.1	41
155	Hydrogenated mesoporous TiO2–SiO2 with increased moderate strong Brönsted acidic sites for Friedel–Crafts alkylation reaction. Catalysis Science and Technology, 2012, 2, 719.	4.1	19
156	Fluorine-planted titanosilicate with enhanced catalytic activity in alkene epoxidation with hydrogen peroxide. Catalysis Science and Technology, 2012, 2, 2433.	4.1	50
157	Measurement of Aluminum–Carbon Distances Using Sâ€RESPDOR NMR Experiments. ChemPhysChem, 2012, 13, 3605-3615.	2.1	59
158	Enhancement of BrÃ,nsted acidity in zeolitic catalysts due to an intermolecular solvent effect in confined micropores. Chemical Communications, 2012, 48, 6936.	4.1	35
159	Room temperature activation of methane over Zn modified H-ZSM-5 zeolites: Insight from solid-state NMR and theoretical calculations. Chemical Science, 2012, 3, 2932.	7.4	157
160	NMRâ€Spectroscopic Evidence of Intermediateâ€Dependent Pathways for Acetic Acid Formation from Methane and Carbon Monoxide over a ZnZSMâ€5 Zeolite Catalyst. Angewandte Chemie - International Edition, 2012, 51, 3850-3853.	13.8	84
161	Influence of acid strength on the reactivity of alkane activation on solid acid catalysts: A theoretical calculation study. Microporous and Mesoporous Materials, 2012, 151, 241-249.	4.4	39
162	Molecular engineering of microporous crystals: (IV) Crystallization process of microporous aluminophosphate AlPO4-11. Microporous and Mesoporous Materials, 2012, 152, 190-207.	4.4	26

#	Article	IF	CITATIONS
163	Theoretical Investigation of the Effects of the Zeolite Framework on the Stability of Carbenium Ions. Journal of Physical Chemistry C, 2011, 115, 7429-7439.	3.1	83
164	BrÃ,nsted/Lewis Acid Synergy in H–ZSM-5 and H–MOR Zeolites Studied by <sup>1</sup> H and <sup>27</sup> Al DQ-MAS Solid-State NMR Spectroscopy. Journal of Physical Chemistry C, 2011, 115, 22320-22327.	3.1	147
165	Boron Environments in B-Doped and (B, N)-Codoped TiO <sub>2</sub> Photocatalysts: A Combined Solid-State NMR and Theoretical Calculation Study. Journal of Physical Chemistry C, 2011, 115, 2709-2719.	3.1	164
166	Acidic Strengths of BrÃ,nsted and Lewis Acid Sites in Solid Acids Scaled by <sup>31</sup> P NMR Chemical Shifts of Adsorbed Trimethylphosphine. Journal of Physical Chemistry C, 2011, 115, 7660-7667.	3.1	104
167	Acid properties of solid acid catalysts characterized by solid-state 31P NMR of adsorbed phosphorous probe molecules. Physical Chemistry Chemical Physics, 2011, 13, 14889.	2.8	204
168	New Insights into Kegginâ€Type 12â€Tungstophosphoric Acid from <sup>31</sup> P MAS NMR Analysis of Absorbed Trimethylphosphine Oxide and DFT Calculations. Chemistry - an Asian Journal, 2011, 6, 137-148.	3.3	42
169	Synthesis of high-silica EU-1 zeolite in the presence of hexamethonium ions: A seeded approach for inhibiting ZSM-48. Journal of Colloid and Interface Science, 2011, 358, 252-260.	9.4	38
170	Acidity of Solid and Liquid Acids Probed by P-31 NMR Chemical Shifts of Phosphine Oxides. Journal of Analytical Science and Technology, 2011, 2, A155-A158.	2.1	5
171	Distance measurement between a spin-1/2 and a half-integer quadrupolar nuclei by solid-state NMR using exact analytical expressions. Journal of Magnetic Resonance, 2010, 206, 269-273.	2.1	61
172	Isomeric Effect on H/D Exchange of Resveratrol Studied by NMR Spectroscopy. Chinese Journal of Chemistry, 2010, 28, 2281-2286.	4.9	5
173	Reactivity of C <sub>1</sub> Surface Species Formed in Methane Activation on Znâ€Modified Hâ€ZSMâ€5 Zeolite. Chemistry - A European Journal, 2010, 16, 14016-14025.	3.3	68
174	Insights into the Dealumination of Zeoliteâ€HY Revealed by Sensitivityâ€Enhanced <sup>27</sup> Al DQâ€MAS NMR Spectroscopy at High Field. Angewandte Chemie - International Edition, 2010, 49, 8657-8661.	3 13.8	173
175	Breaking the T1 Constraint for Quantitative Measurement in Magic Angle Spinning Solid-State NMR Spectroscopy. Journal of the American Chemical Society, 2010, 132, 5538-5539.	13.7	20
176	Combined Solid-State NMR and Theoretical Calculation Studies of BrÃ,nsted Acid Properties in Anhydrous 12-Molybdophosphoric Acid. Journal of Physical Chemistry C, 2010, 114, 15464-15472.	3.1	57
177	<sup>13</sup> C Chemical Shift of Adsorbed Acetone for Measuring the Acid Strength of Solid Acids: A Theoretical Calculation Study. Journal of Physical Chemistry C, 2010, 114, 12711-12718.	3.1	67
178	New Insights into the Effects of Acid Strength on the Solid Acid-Catalyzed Reaction: Theoretical Calculation Study of Olefinic Hydrocarbon Protonation Reaction. Journal of Physical Chemistry C, 2010, 114, 10254-10264.	3.1	41
179	Measurement of hetero-nuclear distances using a symmetry-based pulse sequence in solid-state NMR. Physical Chemistry Chemical Physics, 2010, 12, 9395.	2.8	120
180	Indirect Detection via Spin-1/2 Nuclei in Solid State NMR Spectroscopy: Application to the Observation of Proximities between Protons and Quadrupolar Nuclei. Journal of Physical Chemistry A, 2009, 113, 12864-12878.	2.5	81

#	Article	IF	CITATIONS
181	<sup>19</sup> F Chemical Shift of Crystalline Metal Fluorides: Theoretical Predictions Based on Periodic Structure Models. Journal of Physical Chemistry C, 2009, 113, 15018-15023.	3.1	61
182	Inorganic molecular imprinted titanium dioxide photocatalyst: synthesis, characterization and its application for efficient and selective degradation of phthalate esters. Journal of Materials Chemistry, 2009, 19, 4843.	6.7	92
183	Synthesis of α-layered sodium disilicate and its tribological properties in liquid paraffin. Journal of Materials Chemistry, 2009, 19, 6896.	6.7	14
184	Acidity of sulfated tin oxide and sulfated zirconia: A view from solid-state NMR spectroscopy. Catalysis Communications, 2009, 10, 920-924.	3.3	45
185	Reactivity Enhancement of 2-Propanol Photocatalysis on SO <sub>4</sub> <sup>2â^`</sup> /TiO <sub>2</sub> : Insights from Solid-State NMR Spectroscopy. Environmental Science & Technology, 2008, 42, 5316-5321.	10.0	49
186	<sup>31</sup> P Chemical Shift of Adsorbed Trialkylphosphine Oxides for Acidity Characterization of Solid Acids Catalysts. Journal of Physical Chemistry A, 2008, 112, 7349-7356.	2.5	92
187	Probing the Spatial Proximities among Acid Sites in Dealuminated H-Y Zeolite by Solid-State NMR Spectroscopy. Journal of Physical Chemistry C, 2008, 112, 14486-14494.	3.1	105
188	Theoretical Predictions of <sup>31</sup> P NMR Chemical Shift Threshold of Trimethylphosphine Oxide Absorbed on Solid Acid Catalysts. Journal of Physical Chemistry B, 2008, 112, 4496-4505.	2.6	143
189	Formation, Location, and Photocatalytic Reactivity of Methoxy Species on Keggin 12-H <sub>3</sub> PW <sub>12</sub> O <sub>40</sub> : A Joint Solid-State NMR Spectroscopy and DFT Calculation Study. Journal of Physical Chemistry C, 2008, 112, 15765-15770.	3.1	31
190	Super Hydrophobic Mesoporous Silica with Anchored Methyl Groups on the Surface by a One-Step Synthesis without Surfactant Template. Journal of Physical Chemistry C, 2007, 111, 999-1004.	3.1	42
191	Crystallization of AlPO4-5 Aluminophosphate Molecular Sieve Prepared in Fluoride Medium:Â A Multinuclear Solid-State NMR Study. Journal of Physical Chemistry B, 2007, 111, 7105-7113.	2.6	54
192	Relationship Between 1H Chemical Shifts of Deuterated Pyridinium Ions and BrÃ,nsted Acid Strength of Solid Acids. Journal of Physical Chemistry B, 2007, 111, 3085-3089.	2.6	82
193	Solid-state NMR studies of methanol-to-aromatics reaction over silver exchanged HZSM-5 zeolite. Microporous and Mesoporous Materials, 2007, 98, 214-219.	4.4	34
194	BrÃ,nsted/Lewis Acid Synergy in Dealuminated HY Zeolite:  A Combined Solid-State NMR and Theoretical Calculation Study. Journal of the American Chemical Society, 2007, 129, 11161-11171.	13.7	349
195	A new study on the kinetics of Stöber synthesis by in-situ liquid 29Si NMR. Journal of Sol-Gel Science and Technology, 2007, 42, 13-20.	2.4	12
196	Ammonia Catalyzed Hydrolysis-Condensation Kinetics of Tetraethoxysilane/Dimethyldiethoxysilane Mixtures Studied by 29 Si NMR and SAXS. Journal of Solution Chemistry, 2007, 36, 327-344.	1.2	24
197	Acidity of Mesoporous MoOx/ZrO2and WOx/ZrO2Materials:Â A Combined Solid-State NMR and Theoretical Calculation Study. Journal of Physical Chemistry B, 2006, 110, 10662-10671.	2.6	70
198	Mesoporous MSU materials functionalized with sulfonic group: A multinuclear NMR and theoretical calculation study. Microporous and Mesoporous Materials, 2006, 89, 219-226.	4.4	26

#	Article	IF	CITATIONS
199	Acid sites in mesoporous Al-SBA-15 material as revealed by solid-state NMR spectroscopy. Microporous and Mesoporous Materials, 2006, 92, 22-30.	4.4	110
200	Additional Incorporation of Aluminum into Al-Containing Mesostructure via Hydrothermal Treatment with NaAlO2 Solution. Journal of Porous Materials, 2005, 12, 107-112.	2.6	2
201	Combined DFT Theoretical Calculation and Solid-State NMR Studies of Al Substitution and Acid Sites in Zeolite MCM-22. Journal of Physical Chemistry B, 2005, 109, 24273-24279.	2.6	80
202	Location, Acid Strength, and Mobility of the Acidic Protons in Keggin 12-H3PW12O40:  A Combined Solid-State NMR Spectroscopy and DFT Quantum Chemical Calculation Study. Journal of the American Chemical Society, 2005, 127, 18274-18280.	13.7	130
203	Brönsted and Lewis Acidity of the BF3/γ-Al2O3Alkylation Catalyst as Revealed by Solid-State NMR Spectroscopy and DFT Quantum Chemical Calculations. Journal of Physical Chemistry B, 2005, 109, 13124-13131.	2.6	29
204	Mixed Cationicâ€nonionic Surfactants and pH Adjustment Route to Synthesize Highâ€quality MCMâ€48. Journal of the Chinese Chemical Society, 2004, 51, 49-57.	1.4	8
205	Solid-state MAS NMR detection of the oxidation center in TS-1 zeolite by in situ probe reaction. Journal of Catalysis, 2004, 221, 670-673.	6.2	39
206	Conformation of Surfactant Molecules in the Interlayer of Montmorillonite Studied by <sup>13</sup> C MAS NMR. Clays and Clay Minerals, 2004, 52, 350-356.	1.3	100
207	Using Trimethylphosphine as a Probe Molecule to Study the Acid Sites in Alâ <sup>~,</sup> MCM-41 Materials by Solid-State NMR Spectroscopy. Journal of Physical Chemistry B, 2003, 107, 2435-2442.	2.6	72
208	Solid state NMR study of acid sites formed by adsorption of SO3 onto Î <sup>3</sup> -Al2O3. Chemical Communications, 2003, , 884-885.	4.1	32
209	Variation of sodium coordination during the hydration processes of layered sodium disilicates as studied by 23Na MQMAS and 1H↔23Na CP/MAS NMR spectroscopyElectronic supplementary information (ESI) available: XRD patterns of SKS-5 and SKS-6 samples after different hydration times, and 1H–1H NOESY spectra of SKS-5 and SKS-6 hydrated for six months. See	6.7	11
210	Synthesis of phenyl-MSU-1 and bi-functionalized silica mesophases. Journal of Materials Research, 2002, 17, 431-437.	2.6	10
211	Preferential Occupation of Xenon in Zeolite MCM-22 As Revealed by129Xe NMR Spectroscopy. Journal of Physical Chemistry B, 2001, 105, 9426-9432.	2.6	23
212	MAS NMR Studies on the Dealumination of Zeolite MCM-22. Journal of Physical Chemistry B, 2001, 105, 1770-1779.	2.6	92
213	Surface modification of Î <sup>3</sup> -Al2O3 by sodium ions. Science Bulletin, 2001, 46, 188-193.	1.7	7
214	Roles for Cyclopentenyl Cations in the Synthesis of Hydrocarbons from Methanol on Zeolite Catalyst HZSM-5. Journal of the American Chemical Society, 2000, 122, 4763-4775.	13.7	296
215	"NMR invisible―aluminum species in dealuminated mordenite zeolite: a1H/27 AI TRAPDOR NMR study. Science in China Series B: Chemistry, 1998, 41, 149-155.	0.8	7
216	1H MAS and 1H[23Na] double resonance NMR studies on the modification of surface hydroxyl groups of Î <sup>3</sup> -alumina by sodium. Solid State Nuclear Magnetic Resonance, 1997, 7, 281-290.	2.3	19

#	Article	IF	CITATIONS
217	Acid Sites and Hydration Behavior of Dealuminated Zeolite HZSM-5: A High-Resolution Solid State NMR Study. The Journal of Physical Chemistry, 1995, 99, 15208-15214.	2.9	62
218	Adsorption of Na+ onto γ-alumina studied by solid-state 23Na and 27Al nuclear magnetic resonance spectroscopy. Solid State Nuclear Magnetic Resonance, 1993, 2, 317-324.	2.3	9
219	Insight into Carbocation Induced Nonâ€covalent Interactions in Methanolâ€toâ€olefins Reaction over ZSMâ€5 Zeolite from Solidâ€State NMR Spectroscopy. Angewandte Chemie, 0, , .	2.0	2
220	Identifying Crystallographically Different Siâ€OHâ€Al BrÃ,nsted Acid Sites in LTA Zeolites. Angewandte Chemie, 0, , .	2.0	0